GROUND TRUTH, MAGNITUDE CALIBRATION AND REGIONAL PHASE PROPAGATION AND DETECTION IN THE MIDDLE EAST AND HORN OF AFRICA

Andrew A. Nyblade[1], Richard A. Brazier[1], Aubreya Adams[1], Yongcheol Park[1], Arthur J. Rodgers,[2] and Abdullah Al-Amri[3]

Penn State University[1], Lawrence Livermore National Laboratory[2], and King Saud University[3]

Sponsored by National Nuclear Security Administration
Office of Nonproliferation Research and Development
Office of Defense Nuclear Nonproliferation

Contract Nos. DE-FC52-05NA26602[1] and W-7405-ENG-48[2]

ABSTRACT

In this project, we are exploiting several seismic data sets to improve U.S. operational capabilities to monitor for low yield nuclear tests across the Middle East (including the Iranian Plateau, Zagros Mountains, Arabian Peninsula, Turkish Plateau, Gulf of Aqaba, Dead Sea Rift) and the Horn of Africa (including the northern part of the East African Rift, Afar Depression, southern Red Sea and Gulf of Aden). The data sets are being used to perform three related tasks. (1) We are determining moment tensors, moment magnitudes and source depths for regional events in the magnitude 3.0 to 6.0 range. (2) These events are being used to characterize high-frequency (0.5–16 Hz) regional phase attenuation and detection thresholds, especially from events in Iran recorded at stations across the Arabian Peninsula. (3) We are collecting location ground truth at GT5 (local) and GT20 (regional) levels for seismic events with M > 2.5, including source geometry information and source depths.

Towards meeting these objectives, seismograms from earthquakes in the Zagros Mountains recorded at regional distances have been inverted for moment tensors, which have then been used to create synthetic seismograms to determine the source depths of the earthquakes via waveform matching. The source depths have been confirmed by modeling teleseismic depth phases recorded on Global Seismographic Network (GSN) and International Monitoring System (IMS) stations. Early studies of the distribution of seismicity in the Zagros region found evidence for earthquakes in the upper mantle. But subsequent relocations of teleseismic earthquakes suggest that source depths are generally much shallower, lying mainly within the upper crust. All of the regional events studied so far nucleated within the upper crust, and most of the events have thrust mechanisms. The source mechanisms for these events are being used to characterize high-frequency (0.5–16 Hz) regional phase attenuation and detection thresholds for broadband seismic stations in the Arabian Peninsula, including IMS stations and stations belonging to the Saudi Arabian National Digital Seismic Network.

To improve event locations, source mechanisms and attenuation estimates, new regional P and S wave velocity models of the upper mantle under the Arabian Peninsula have also been developed using data from teleseismic events recorded at stations within the Arabian Peninsula and Horn of Africa. These models show slower-than-average velocities within the lithsopheric mantle under the entire Arabian Shield. However, at sublithospheric mantle depths, the low velocity region appears to be localized beneath the western side of the Arabian Shield.

OBJECTIVE

The objective of this effort is to determine ground truth source parameters (depth, moment, focal mechanism) for earthquakes in the Middle East. For this reporting period we focused on events in the Zagros Mountains of Iran and used unique broadband waveforms from regional stations. Source moments are being used to calibrate coda wave moment magnitudes (Mayeda et al., 2003) and to model high-frequency regional body-wave amplitude spectra with the magnitude-distance amplitude correction (MDAC) methodology (Walter and Taylor, 2002). In subsequent periods, we will determine models of the propagation characteristics, including attenuation, of high-frequency regional phases. These models will then be used to estimate detection thresholds by comparing model-based predictions of signal amplitudes to background noise levels. To help in this effort, we have also developed new velocity models of the upper mantle beneath the Arabian Peninsula.

RESEARCH ACCOMPLISHED

Introduction

In this project, we are exploiting unique and open source seismic data sets to improve seismic monitoring for the Middle East (including the Iranian Plateau, Zagros Mountains, Arabian Peninsula, Turkish Plateau, Gulf of Aqaba, Dead Sea Rift) and the Horn of Africa (including the northern part of the East African Rift, Afar Depression, southern Red Sea and Gulf of Aden). Broadband waveform data sets are being used to perform three related tasks. (1) We are determining moment tensors, moment magnitudes and source depths for regional events in the magnitude 3.0 to 6.0 range.(2) These events are being used to characterize high-frequency (0.5–16 Hz) regional phase attenuation and detection thresholds, especially from events in Iran recorded at stations across the Arabian Peninsula. (3) We are collecting location ground truth at GT5 (local) and GT20 (regional) levels for seismic events with M >2.5, including source geometry information and source depths.

The results of this research will enhance monitoring capabilities within the study region by improving our understanding of high frequency regional phase attenuation and how this attenuation affects detection thresholds. Accurate hypocentral locations of M >2.5 seismic events are needed to construct travel time correction surfaces, which are of fundamental importance to ground-based nuclear explosion monitoring.

Towards meeting these objectives, seismograms from earthquakes in the Zagros Mountains recorded at regional distances have been inverted for moment tensors, which have then been used to create synthetic seismograms to determine the source depths of the earthquakes via waveform matching. The source depths have been confirmed by modeling teleseismic depth phases recorded on GSN and IMS stations. Early studies of the distribution of seismicity in the Zagros region found evidence for earthquakes in the upper mantle. But subsequent relocations of teleseismic earthquakes suggest that source depths are generally much shallower, lying mainly within the upper crust. All of the regional events studied so far nucleated within the upper crust, and most of the events have thrust mechanisms. The source mechanisms for these events are being used to characterize high-frequency (0.5–16 Hz) regional phase attenuation and detection thresholds for broadband seismic stations in the Arabian Peninsula, including IMS stations and stations belonging to the Saudi Arabian National Digital Seismic Network.

To improve event locations, source mechanisms and attenuation estimates, new regional P- and S-wave velocity models of the upper mantle under the Arabian Peninsula have also been developed using data from teleseismic events recorded at stations within the Arabian Peninsula and Horn of Africa. These models show slower-than-average velocities within the lithsopheric mantle under the entire Arabian Shield. However, at sublithospheric mantle depths, the low velocity region appears to be localized beneath the western side of the Arabian Shield.

Background

The Arabian Shield consists of late Proterozoic crystalline basement overlain by Tertiary and Quaternary volcanic rocks in some places. The breakup of the Arabian Plate from Africa initiated at about 30–35 Ma,

with the formation of the Red Sea-Gulf of Aden rift system (Coleman and McGuire, 1988). Volcanism was widespread between 30 and 12 Ma, and uplift of the Arabian Shield occurred at about 13 Ma (Coleman and McGuire, 1988). The volcanism and uplift are thought to be related to the presence of hot upper mantle (Camp and Roobol, 1992). The uplifted Arabian Shield contains two major features: one is the Makkah-Madinah-Nafud (MMN) volcanic line in the south and the other is the Ha'il-Rutbah Arch in the north (Figure 1). The MMN volcanic line, extending north-south, has been the major site of volcanism in Saudi Arabia over the past 10 Ma and the Ha'il-Rutbah Arch has been the site of several periods of uplift (Camp and Roobol, 1992).

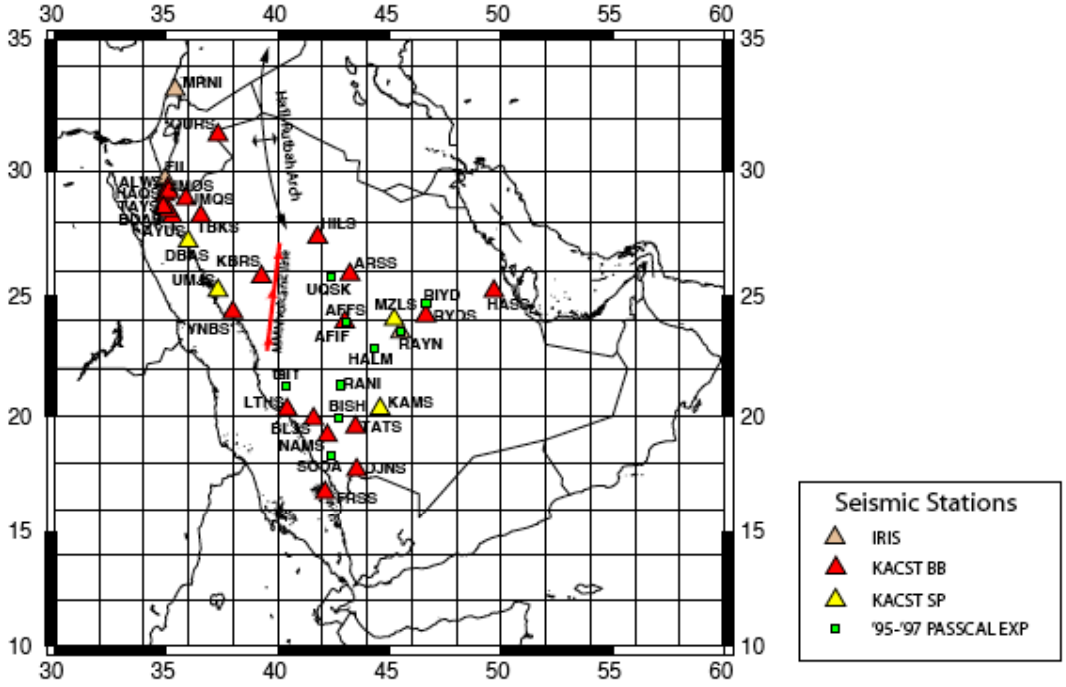

Figure 1. Map showing seismic stations in the Arabian Peninsula used in this study. KACST stations belong to the Saudi Arabia Digital National Seismic network.

The Zagros Mountain Belt, one of the world's most seismically active mountain ranges, marks the convergent boundary between the Arabian and Eurasian plates in southwestern Iran (Figure 2). The upper 11 km of the crust consists of folded sedimentary layers, while the lower 36 km of the crust are composed of faulted crystalline basement rock. The most prominent fault exposed at the surface is the Zagros Main Thrust, which marks the northern extent of seismicity associated with the Zagros Mountains and separates the Zagros Mountains from the Central Iranian Plateau. The Moho dips to the northeast from a depth of 40 km beneath the Persian Gulf to a maximum depth of approximately 65–70 km beneath the Zagros Main Thrust (Paul et al., 2006). Early studies of the distribution of seismicity in the Zagros region found evidence for earthquakes in the upper mantle (Nowroozi, 1971; Bird et al., 1975). Subsequent recalculations of teleseismic earthquakes indicated that source depths were much shallower, lying within the upper crust (Maggi et al., 2000, 2002).

Zagros Earthquakes

Source depths and focal mechanisms for six well-studied events have been obtained (Table 1). A grid search method was used to determine the source parameters of each event. First, regional waveforms for each event were inverted for a moment tensor over a range of potential source depths. Synthetic seismograms were then computed using a reflectivity code for each source mechanism and compared to observed waveforms. In addition to the KACST and Program for the Array Siesmic Studies of the continental Lithosphere (PASSCAL) stations, data recorded at regional distances on open stations to the north and east were used, providing fairly good azimuth ray coverage for each event. The quality of the

visual fit between the synthetic and observed waveforms, along with the root mean square error, was used to determine the best-fitting focal mechanism and associated source depth.

In addition, to help constrain focal depths, teleseismic depth phases from open stations in the 30 to 90 degree distance range have been modeled using the focal mechanism obtained from the grid search at a particular depth.

Figure 2. Colored topography map of the Middle East showing the location of the main plates and the Zagros Mountains.

The locations of the events are shown in Figure 3. Most of the events studied occurred within the central portion of the Zagros Mountains where there are the best constraints on crustal structure provided by receiver function and gravity studies. Figures 4a and 4b summarize graphically the results for two of the events, and serve to illustrate the quality of the waveform fits that we have obtained. Source depths for the events are within the upper crust.

Table 1a. Source parameters for well-studied events in the Zagros Mountains. Event letters are the same as in Figure 3.

Event Letter	Event ID Number	Date MM/DD/YYYY	Time	M0	Mw	Mw CMT	Strike/Dip/Rake (Plane 1)	Strike/Dip/Rake (plane 2)
A	9962	11/13/1998	13:01:10	1.35E+24	5.4	5.4	144.21/65.33/120.95	269.05/38.80/41.76
B	1320614	10/31/1999	15:09:40	7.13E+23	5.2	5.2	158.09/69.17/102.39	306.38/24.10/60.58
C	4070289	03/01/2000	20:06:29	1.93E+23	4.8	5.0	298.57/49.98/134.73	61.56/57.04/50.03
D	1582024	02/17/2002	13:03:53	1.01E+24	5.3	5.5	109.24/10.24/76.99	302.46/80.03/92.33
E	4357281	07/10/2003	17:40:16	4.64E+24	5.7	5.6	343.19/6.42/35.13	218.22/86.31/95.26
F	1559906	04/13/2001	01:04:27	3.93E+23	5	5.1	96.81/14.85/134.62	231.21/79.49/79.45

Table 1b. Moment tensors and source depth for well-studied events in the Zagros Mountains. Event letters are the same as in Figure 3.

Event Letter	Mxx	Mxy	Mxz	Myy	Myz	Mzz	Depth
A	8.67E+10	3.73E+10	-4.49E+09	5.16E+09	-9.42E+10	-9.19E+10	12 (+-2)
B	2.35E+10	1.97E+10	-1.13E+10	2.72E+10	-5.13E+10	-5.08E+10	12 (+-2)
C	1.79E+10	2.01E+08	-1.97E+09	-4.28E+09	1.04E+10	-1.36E+10	9 (+-3)
D	2.85E+10	1.84E+10	7.94E+10	2.29E+09	5.09E+10	-3.08E+10	4 (+-2)
E	4.01E+08	1.31E+10	2.90E+11	8.04E+10	-3.54E+11	-8.08E+10	39 (+10/- 15)
F	1.52E+10	5.69E+08	2.55E+10	2.08E+09	-2.50E+10	-1.73E+10	8 (+-3)

In addition to the six well-studied events in the region of the Zagros where crustal structure is best known, we also have preliminary moment tensor solutions for several other events spread throughout the Zagros Mountains. Teleseismic depth phases for these events have been identified on short-period data from the Norwegian Seismic Array (NORSAR), but they have not yet been modeled to determine source depth. The preliminary results for these events are provided in Table 2.

Table 2a. Source parameters for other events in the Zagros Mountains

Event Num.	Event ID Number	Date MM/DD/YYYY	Time	M0	Mw	Mw CMT	Strike/Dip/Rake (Plane 1)	Strike/Dip/Rake (plane 2)
1	6307	04/19/1997	05:53:14	1.36E+24	5.4	5.5	177.91/9.16/251.53	16.60/81.31/87.08
2	6758	10/20/1997	06:09:04	9.64E+23	5.3	5.6	129.15 /0.60/120.46	278.68/ 89.49/89.7
3	8893	07/10/2003	19:40:27			5.9	315.51/5.86/-4.29	49.77/89.56/264.16
4	4357280	02/17/2002	17:06:37	7.52E+24	5.9	5.9	67.7/1.83/142.71	194.97/88.89/88.54

Table 2b. Moment tensors and source depth for other events in the Zagros Mountains

Event Num.	Mxx	Mxy	Mxz	Myy	Myz	Mzz	Depth
1	1.89E+10	1.64E+10	7.23E+10	-5.18E+10	-1.81E+11	3.29E+10	4 (+-2)
2	5.58E+09	2.69E+09	9.5E+10	-8.20E+09	1.46E+10	2.62E+09	4 (+-2)
3	-2.32E+10	-8.2E+08	1.53E+09	-1.60E+09	-1.32E+10	7.27E+10	5 (+-2)
4	9.23E+10	1.00E+10	1.89E+11	-1.84E+10	-7.23E+11	-7.39E+10	5 (+-2)

The focal depth of earthquakes can affect the excitation of regional phases, particularly the guided Lg phase, which is composed of higher mode surfaces waves whose amplitudes are strongly depth dependent. The source parameters determined above can be used to infer how focal mechanism and depth might impact regional phase S-wave generation and this might in turn impact P/S discriminants. Two nearby events (A and H) were recorded at station HILS on the northern Arabian Shield. Event A is the same event as in Table 1 and Figure 3. Event H was reported in Nyblade et al. (2006) for this project. These events had similar magnitudes (5.4 versus 5.7) and although are both thrust mechanisms their strikes are slightly different. The high-frequency (0.5–5 Hz) response of these events are shown in Figure 5. Note that Lg is weaker with respect to the Pn for the deeper event (H), making the Pn/Lg ratio discriminant more explosion-like for this event. This suggests a possible depth-dependence of the Lg amplitude (and Pn/Lg ratio discriminant). Alternatively, the further event (H) may be located in a region of thicker crust, which leads to disruption of the crustal waveguide along the path to HILS. Both explanations would cause additional scatter in body-wave discriminants, compounding discrimination strategies. These observations will be explored in further work on this project.

Body Wave Tomography

Upper mantle structure strongly impacts the propagation of regional Pn and Sn phases. We report velocity structure of the upper mantle reported from teleseismic P and S body waves. While this study resolves deep upper mantle structure, there are likely relationships with structure directly below the crust. To investigate upper mantle structure under the Arabian Shield, measured and inverted relative travel times from stations in Arabia. We augmented the KACST data with delay times measured from permanent stations in the region (RAYN, EIL and MRNI) and the 1995-7 Saudi Arabian PASSCAL Experiment data set. Figure 1 shows the locations of seismic network used in this study. We computed travel time differences for two nearly co-located stations (AFFS and AFIF in Figure 1) between KACST and the PASSCAL networks in order to investigate possible biases between these data sets before combining all delay times from different seismic networks. We sorted events recorded on the common stations by back azimuth and distance and measured P-wave travel time residuals from arrival times subtracted from a theoretical travel time. The trends of the residuals with back-azimuth and distance are very similar and indicate no bias between the travel time residuals for the common stations.

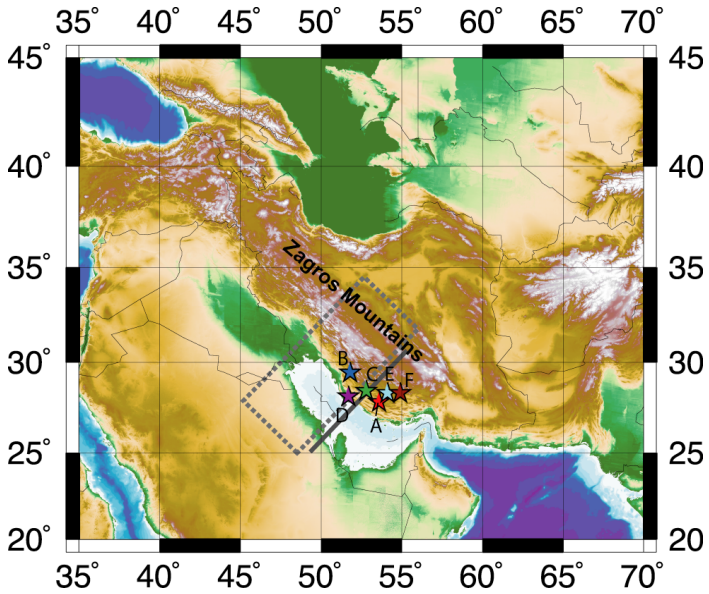

Figure 3. Map of the Zagros Mountains and Persian Gulf showing the locations of earthquakes studied. Letters correspond to the events in Table 1. The grey box shows area where crustal thickness has been constrained using gravity data and the white line shows were crustal thickness has been imaged using receiver functions.

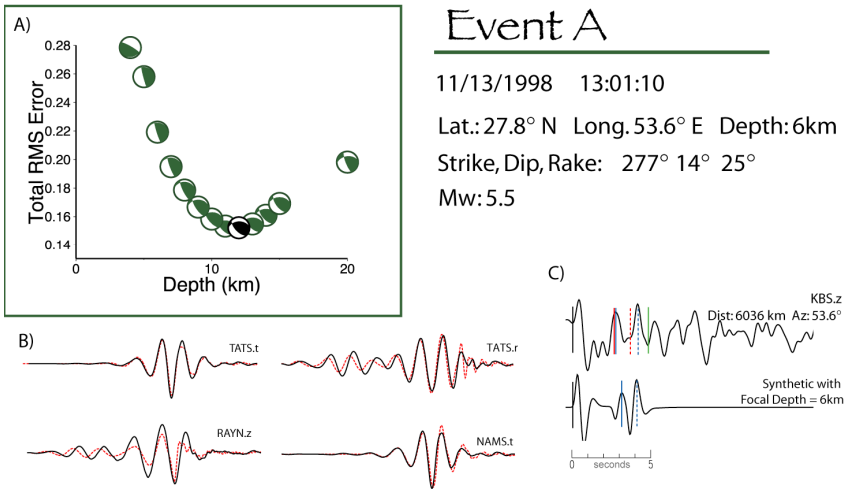

Figure 4a. Example result for one of the well-studied earthquakes illustrating the method used for obtaining source parameters and the quality of the waveform fits. A) Plot of focal depth vs. error showing a source depth of about 12 km. B) Long period regional displacement waveforms (black line) and synthetics (red dotted line) for a number of stations. C) Short period teleseismic waveforms showing depth phases. The top trace is the data and the bottom one is a synthetic. Solid blue line is our pP pick and the dotted blue line is our sP pick. The other colored lines show pP and sP picks from various catalogs. The short period depth phases give a source depth of 6 km, which is not inconsistent with the source depth obtained from the grid search, indicating a broad minimum in the RMS error (see A) between about 6 and 15 km depth.

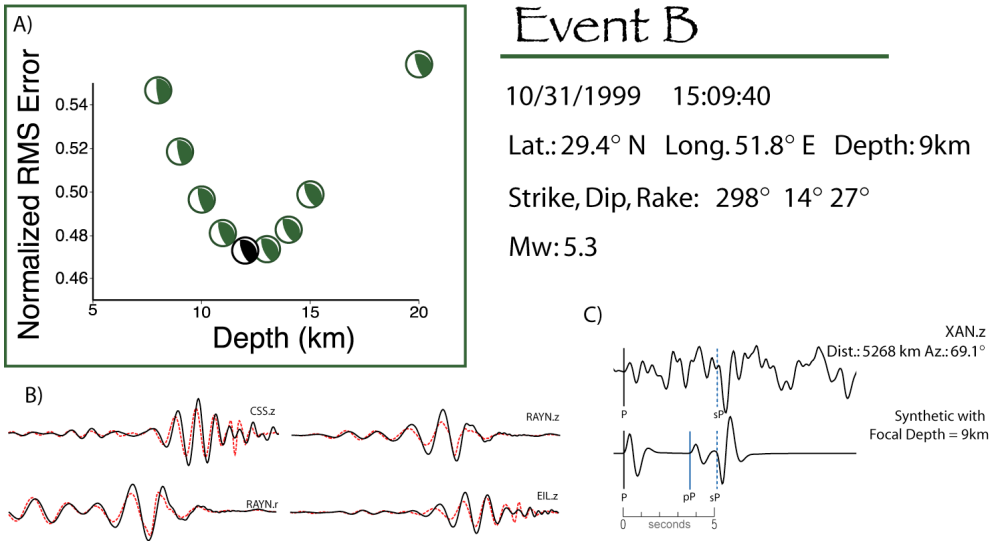

Figure 4b. Example result for one on the well-studied earthquakes illustrating the method used for obtaining source parameters and the quality of the waveform fits. A) Plot of focal depth vs. error showing a source depth of about 12 km. B) Long period regional displacement waveforms (black line) and synthetics (red dotted line) for a number of stations. C) Short period teleseismic waveforms showing depth phases. The top trace is the data and the bottom one is a synthetic. Solid blue line is our pP pick and the dotted blue line is our sP pick. The short period depth phases give a source depth of 9 km, which in not inconsistent with the source depth obtained from the grid search, indicating a broad minima in the RMS error (see A) between about 9 and 15 km depth.

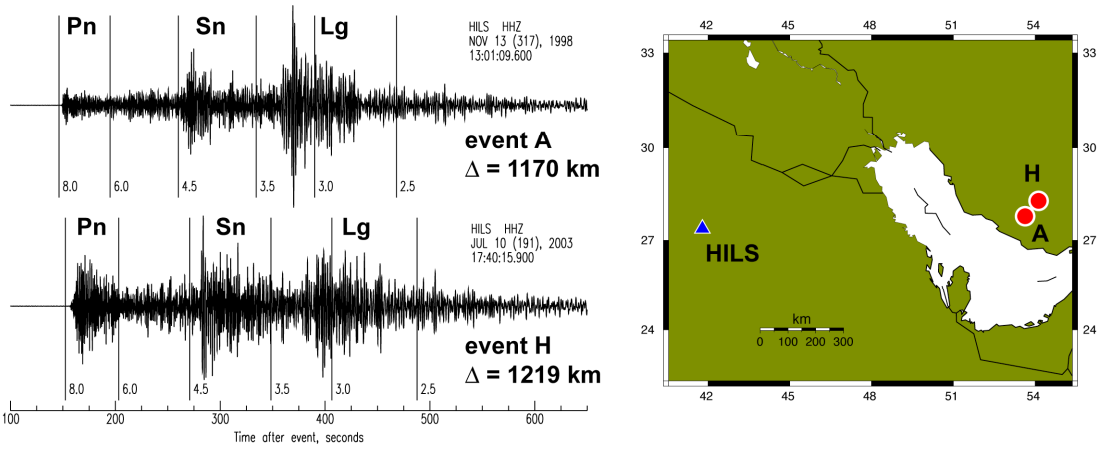

Figure 5. (left) Vertical component waveforms (filtered 0.5–5 Hz) for events A (top) and H (bottom) at station HILS (Al Hail, Saudi Arabia). (right) These events are closely located with event H slightly further away.

For the data sets, we computed relative arrival time residuals using a multi-channel cross-correlation method (VanDecar and Crosson, 1990) and inverted for a three dimensional velocity model using the method of VanDecar (1991). For the inversion, we parameterized travel time slowness using a grid of knots comprised of 34 knots in depth, 56 knots latitude between 12.0° N and 37.0° N and 56 knots in longitude between 29.5° E and 55.0° E. The horizontal knot spacing is one third of a degree, and the vertical knot spacing is 25 km in the inner region of the seismic array (17.4° N-30.7° N, 35.5° E-48.5° E, and 0–200 km depth). We used the IASP91 model (Kennett and Engdahl, 1991) as the initial model for the inversion.

Results for the P-wave Tomography

We used 401 earthquakes resulting in 3,416 ray paths with P- and PKP-wave arrivals. The majority of the events are located in the western Pacific Rim between back azimuths of 15 and 150 degrees, but the events are distributed over a wide range of back azimuths. The waveforms were filtered with a zero-phase two-pole Butterworth filter between 0.5 to 2 Hz before the relative travel time residuals were computed. The multi-channel cross-correlation (MCCC) procedure was performed over a three-second window on the filtered data. A final model was selected by investigating the way in which changes in regularization levels (flattening and smoothing values) affect the reduction in travel time residuals. To determine a preferred model, 2,000 iterations of the conjugate gradient procedure are performed with several different pairs of flattening and smoothing values. For our preferred model, we have chosen a model with the values of 1,600 for flattening and 3200 for smoothing.

Figure 6 shows depth slices (a–d) and vertical cross-sections (e and f) through the model. A preliminary interpretation of these features would suggest that low velocities beneath the Gulf of Aqaba and southern Arabian Shield and Red Sea are related to mantle upwelling and seafloor spreading. Low velocities beneath the northern Arabian Shield may be related to volcanic centers. The origins of the low velocity features near the eastern edge of the Arabian Shield and western edge of Arabian Platform are unknown.

Results from the S-Wave Tomography

For the S-wave model, we used 201 earthquakes resulting in 1,602 ray paths with S and SKS-wave arrivals. Although the total number of rays for the S-wave model is half of the rays for the P-wave model, the event distribution shows better coverage of back azimuth. The signal processing procedures for the S-wave data are exactly the same as for the P-wave data, but traces were filtered over a lower frequency band (0.04 to 0.1 Hz), and relative arrival time residuals were computed by the MCCC method using fifteen-second window. As a result we could use the short-period stations for the P-wave analysis, but were limited to data from the broadband stations for the S-wave model. The first order velocity variations seen in the S model are similar to the P model, and therefore we do not show the S-wave model here.

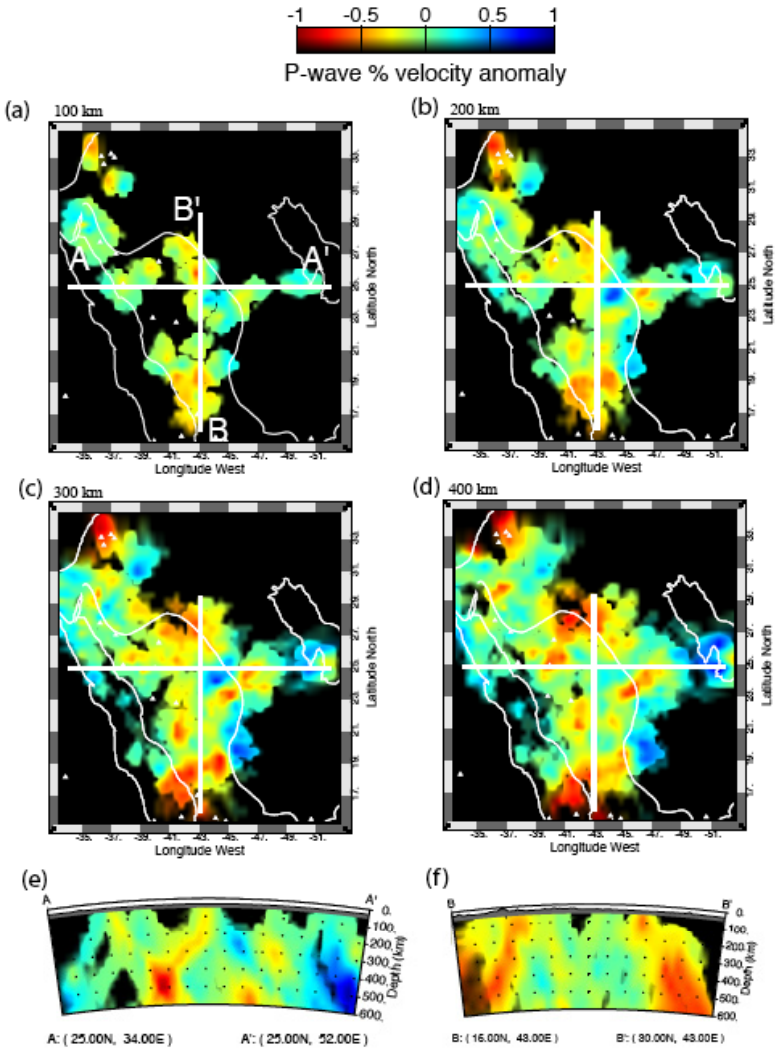

Figure 6. Results of P-wave tomography. (a–d) Depth slices through the model at depths of 100, 200, 300, and 400 km. (e–f) Vertical slices through the model along E-W (e) and N-S (f) profiles denoted with white lines in a–d.

CONCLUSIONS AND RECOMMENDATIONS

We reported progress on the determination of ground truth source parameters (focal depths and mechanisms, seismic moments) for earthquakes in the Zagros Mountains. These moments can be used to calibrate coda wave magnitudes and to model high frequency regional phase amplitude spectra with the MDAC methodology. We will explore the effect of location and focal depth on regional phase amplitudes and discriminants and estimate propagation properties (including attenuation, quality factors). Regional phase propagation models (derived from the MDAC methodology) will be developed to improve understanding of high frequency body-wave discriminants and amplitude detection thresholds in the Middle East.

ACKNOWLEDGEMENTS

The facilities of the IRIS Data Management System, and specifically the IRIS Data Management Center, were used for access to waveform and metadata required in this study.

REFERENCES

Bird, P., M. N. Toksoz, and N. H. Sleep (1975). Thermal and mechanical models of continent-continent convergence zones, *J. Geophys. Res*. 80: 4405–4416.

Camp, V. E. and M. J. Roobol (1992). Upwelling asthenosphere beneath western Arabia and its regional implications, *J. Geophys. Res.* 97: 15255–15271.

Coleman, R. G. and A. V. McGuire (1988). Magma systems related to the Red-Sea opening, *Tectonophysics* 150: 77–100.

Kennett, B. and E. R. Engdahl (1991). Travel times for global earthquake location and phase identification, *Geophys. J. Int.* 105: 429–465.

Maggi, A., J. Jackson, K. Priestley, and C. Baker (2000). A re-assessment of focal depth distributions in southern Iran, the Tien Sha and northern India: Do earthquakes really occur in the continental mantle?, *Geophys. J. Int.* 143: 629–661.

Maggi, A., K. Priestley, and J. Jackson (2002). Focal depths of moderate to large earthquakes in Iran. *Journal of Seismology and Earthquake Engineering* 4: 1–10.

Mayeda, K., A. Hofstetter, J. O'Boyle, and W. Walter (2003). Stable and transportable regional magnitudes based on coda-derived moment-rate spectra, *Bull. Seism. Soc. Am*. 93: 224–239.

Nowroozi, A. A. (1971). Seismotectonics of the Persian Plateau eastern Turkey, Caucasus, and Hindu-Kush Regions, *Bull. Seism. Soc. Am*. 61: 317–342.

Nyblade, A., A. Adams, R. Brazier, Y. Park, and A. Rodgers (2006). Ground truth, magnitude calibration and regional Phase propagation and detection in the Middle East and Horn of Africa, in *Proceedings of the 28th Seismic Research Review: Ground-Based Nuclear Explosion Monitoring Technologies,* LA-UR-06-5471, Vol. 1, pp. 156–165.

Paul, A., A. Kaviani, D. Hatzfeld, J. Vergne, and Mohammad Moktari (2006). Seismological evidence for crustal scale thrusting in the Zagros mountain belt, *Geophys. J. Int.*(submitted).

VanDecar, J. C. (1991). Upper mantle structure of the Cascadia subduction zone from non-linear teleseismic travel time inversion, Ph. D. thesis, Univ. of Washington, Seattle, WA.

VanDecar, J. C. and R. S. Crosson (1990). Determination of teleseismic relative phase arrival times using multi-channel, cross-correlation and least squares, *Bull. Seism. Soc. Am.* 80: 150–169.

Walter, W. and S. Taylor (2002). A revised magnitude and distance amplitude correction (MDAC2) procedure for regional seismic discriminants, Lawrence Livermore National Laboratory technical report, UCRL-ID-146882.